ARTICLE NO. 78-1332R

# C/STOL Flight in Wind Disturbed by the Presence of Buildings

Walter Frost* and Ravi Reddy†
*University of Tennessee Space Institute, Tullahoma, Tenn.*

Bill Crosby‡
*Arnold Engineering and Development Center, Tullahoma, Tenn.*

and

Dennis W. Camp§
*NASA George C. Marshall Space Flight Center, Huntsville, Ala.*

**This paper investigates the behavior of winds about block geometries characteristic of building shapes and of the flight performance of aircraft with characteristics of a DC-8 and a DHC-6 as they fly through the wind fields. The three-degrees-of-freedom, nonlinear, longitudinal equations of motion for the aircraft are written to include two-dimensional variable winds and wind shear components. The paper also presents a discussion of the influence of those terms in the equations of motion which explicitly contain effects due to wind shear. Also included is a study of the aircraft's flight paths over the obstacles with both a fixed stick and an automatic landing system.**

## Nomenclature

$\bar{c}$ = wing mean aerodynamic chord
$C_D$ = drag coefficient, $L/(1/2\rho V_a^2 s)$
$C_L$ = lift coefficient, $L/(1/2\rho V_a^2 s)$
$C_m$ = moment coefficient, $M/(1/2\rho V_a^2 s\bar{c})$
$D$ = drag force
$D_i$ = dimensionless constants
$D_1 = qhs/m$
$D_2 = gh/V_o^2$
$D_3 = 0.0$
$D_4 = \bar{c}/2h$
$D_5 = qs\bar{c}h^2/g_c I_{yy}$
$D_6 = g_c F_T h/mV_o^2$
$D_7 = L_T h^2/V_o^2 I_{yy}$
$F_T$ = thrust of the engines
FRL = fuselage reference line
$g$ = magnitude of the acceleration of gravity
$H$ = building height
$h$ = initial altitude
$I_{yy}$ = pitch moment of inertia
$K$ = variable gain constant
$L$ = lift force
$L_T$ = effective moment arm of the thrust vector
$m$ = aircraft mass
$mg$ = gravitational force
$M$ = pitching moment
$\dot{q}$ = time derivative of the pitching rate $q$
$s$ = wing area
$u_*$ = friction velocity
$V$ = dimensionless magnitude of the aircraft velocity relative to the Earth
$V_a$ = dimensionless magnitude of the aircraft velocity relative to the air mass
$\mathbf{V}$ = dimensionless velocity vector relative to the Earth
$\mathbf{V}_a$ = dimensionless velocity vector relative to the air mass
$W_x$ = wind speed horizontal to ground
$W_z$ = wind speed vertical to ground
$x$ = dimensionless distance parallel to the surface of the Earth
$z$ = dimensionless distance perpendicular to the surface of the Earth (positive downward)
$z_o$ = surface roughness
$\alpha$ = angle of attack
$\delta$ = angle between $\mathbf{V}_a$ and $\mathbf{V}$
$\delta_E$ = elevator angle, positive up
$\delta_T$ = angle between the thrust vector and the fuselage reference line (FRL)
$\gamma$ = angle between $\mathbf{V}$ and $x$-axis (flight path angle)
$\gamma'$ = angle between $\mathbf{V}_a$ and $x$-axis (pitch angle)
$(\dot{})$ = refers to the derivative with respect to time

## Wind Fields about Bluff Geometries

OPERATIONS of C/STOL aircraft in the vicinity of buildings may become hazardous due to complex flow-fields created by surface winds passing over the buildings.[1] The two characteristic building geometries considered are a long, low, two-dimensional building which is simulated as a forward-facing step and a long, rectangular, cross section, block geometry. Wind fields about the bluff geometries illustrated in Fig. 1 have been computed by solving the two-dimensional, incompressible, Navier-Stokes equations. Turbulence was modeled in the solution with the two-equation model that includes a transport equation for the turbulence length scale. Details of these solutions are given by Bitte and Frost[2] and Shieh, Frost, and Bitte.[3] Figure 2 shows typical wind fields over the forward-facing step and over the block geometry, respectively. The influence of these wind fields on a STOL or CTOL aircraft passing over the building or landing upon the top of the building is investigated by solving the three-degrees-of-freedom, nonlinear equations of motion for the aircraft with the computed wind fields as inputs.

Presented as Paper 78-1332 at the AIAA Atmospheric Flight Mechanics Conference, Palo Alto, Calif., Aug. 7-9, 1978; submitted Nov. 27, 1978; revision received April 17, 1978. 

Index categories: Handling Qualities, Stability and Control; Simulation; Atmospheric and Space Sciences.

*Director of Atmospheric Science Division. Also President, FWG Associates, Inc., Tullahoma, Tenn. Member AIAA.

†Research Assistant.

‡Project Engineer, von Karman Gas Dynamics Facility. Member AIAA.

§Research Engineer, Atmospheric Science Div., Space Sciences Laboratory.

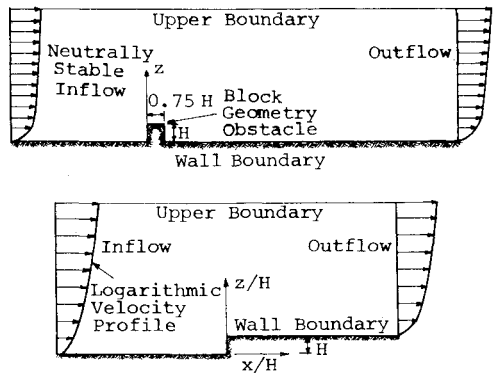


**Fig. 1 Typical bluff geometries considered to simulate buildings.**

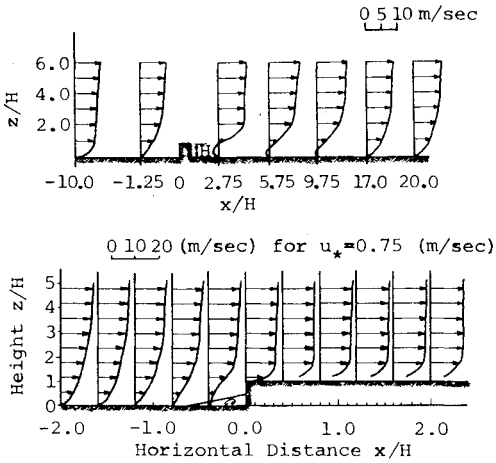


**Fig. 2 Typical wind fields about simulated buildings.**

## Governing Equations of Motion

The aircraft is modeled as a point mass, and a force balance perpendicular and parallel to the ground speed velocity vector (Fig. 3) is employed to derive the following equations:

$$\dot{V} = -D_1(C_D\cos\delta + C_L\sin\delta)V_a^2 - D_2\sin\gamma + D_6F_T\cos(\delta_T+\alpha) \tag{1}$$

$$\dot{\gamma} = [D_1V_a(C_L\cos\delta - C_D\sin\delta) - D_2\cos\gamma + D_6F_T\sin(\delta_T+\alpha)]/V \tag{2}$$

where Fig. 3 defines the nomenclature. A moment balance gives

$$\dot{q} = D_7F_T + D_5V_a^2C_m \tag{3}$$

with the remaining equations making up the complete set:

$$V_a = [(\dot{x}-W_x)^2 + (\dot{z}-W_z)^2]^{1/2} \tag{4}$$

$$V = W_x\cos\delta - W_z\sin\gamma + [(W_z\sin\gamma - W_x\cos\gamma)^2 + V_a^2 - (W_x^2+W_z^2)]^{1/2} \tag{5}$$

$$\sin\delta = (W_x\sin\gamma + W_z\cos\gamma)/V_a \tag{6}$$

$$\dot{\alpha}' = q - D_1C_LV_a - [D_2\cos\gamma' + D_6F_T\sin(\delta_T+\alpha') + (\dot{W}_x\sin\gamma' + \dot{W}_z\cos\gamma')]/V \tag{7}$$

$$\dot{W}_x = \frac{\partial W_x}{\partial t} + V\left(\frac{\partial W_x}{\partial x}\cos\gamma - \frac{\partial W_x}{\partial z}\sin\gamma\right) \tag{8}$$

$$\dot{W}_z = \frac{\partial W_z}{\partial t} + V\left(\frac{\partial W_z}{\partial z}\cos\gamma - \frac{\partial W_z}{\partial z}\sin\gamma\right) \tag{9}$$

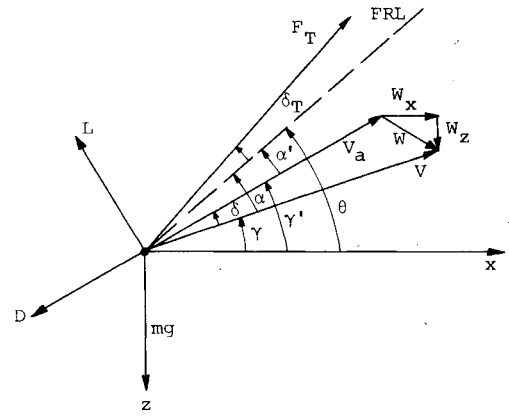


**Fig. 3 Relationship between the forces acting on a point mass aircraft.**

Inspection of the equations shows that wind shear enters explicitly only in Eq. (7). The term $\dot{W}_x\sin\gamma' + \dot{W}_x\cos\gamma'$ in this equation demonstrates that passing through a varying wind field results in a contribution to the rate of change in angle of attack. Of course, variation in wind enters Eqs. (1) and (2) indirectly through $V_a$ and $\delta$ [see Eqs. (4) and (6)]. The aerodynamic coefficients $C_L$, $C_D$, and $C_m$ used in the analysis are those characteristic of either a DC-8 or a DHC-6[4] and are given in terms of the stability derivatives by

$$C_L = C_{L_o} + C_{L_\alpha}\alpha' + C_{L_{\delta_E}}\delta_E + \frac{\bar{c}q}{2V_a}C_{L_q} + \frac{\bar{c}\dot{\alpha}'}{2V_a}C_{L_{\dot{\alpha}}} + \Delta C_{L_{GE}}$$

$$C_D = C_{D_o} + C_{D_\alpha}\alpha' + C_{D_{\alpha^2}}\alpha'^2 + \Delta C_{D_{GE}}$$

$$C_m = C_{m_o} + C_{m_\alpha}\alpha' + C_{m_{\delta_E}}\delta_E + \frac{\bar{c}q}{2V_a}C_{m_q} + \frac{\bar{c}\dot{\alpha}'}{2V_a}C_{m_{\dot{\alpha}}} + \Delta C_{m_{GE}} \tag{10}$$

If the equations of motion are written in terms of airspeed $V_a$ and pitch angle relative to the direction of $V_a$ for a coordinate system with $x$ aligned along $V_a$, one obtains

$$\dot{V}_a = -D_1V_a^2C_D - D_2\sin\gamma' + D_6\cos(\delta_T+\alpha') - \dot{W}_x\cos\gamma' - \dot{W}_z\sin\gamma' \tag{11}$$

$$\dot{\gamma}' = [D_1C_LV_a^2 - D_2\cos\gamma' + D_6F_T\sin(\delta_T+\alpha') + \dot{W}_x\sin\gamma' + \dot{W}_z\cos\gamma']/V_a \tag{12}$$

In these equations, wind shear appears explicitly when $\dot{W}_x$ and $\dot{W}_z$ are introduced through Eqs. (8) and (9).

### Discussion of the Equations of Motion

It is frequently reported that the influence of wind shear will have particularly strong effects on STOL aircraft because of their slow landing speed and steep flight paths. To investigate the significance of this statement, the various terms which explicitly contain wind effects in the equation of motion are examined for CTOL and STOL aircraft. Examination of Eqs. (11) and (12) indicates that there is a contribution to the relative airspeed acceleration and to the pitch rate from the direct entrance of wind shear into the last term on the right-hand side of the equations.

One can isolate these terms and compare their relative magnitude for different types of airplanes under different glide slopes and landing speeds. The contribution $\dot{V}_a$ and $\dot{\gamma}'$ of the wind shear terms thus isolated are given in Eqs. (13)

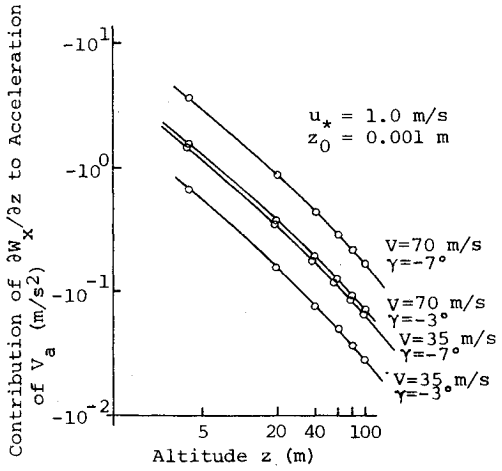


Fig. 4 Contribution of wind shear term to the relative airspeed acceleration.

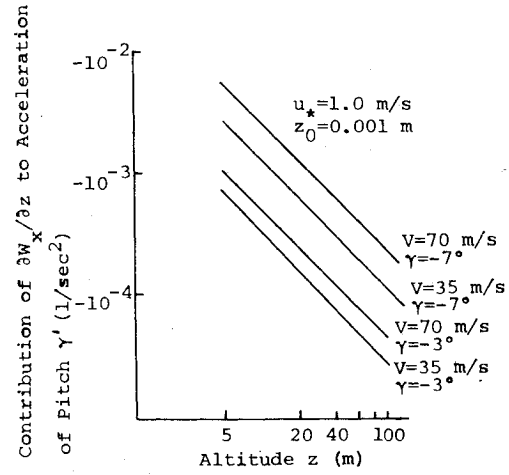


Fig. 5 Contribution of wind shear to change in $\gamma'$.

and (14) below:

$$\Delta\dot{V}_a = -\frac{\partial W_x}{\partial z} V_a \left[ \frac{V}{V_a} \sin\gamma \left( \frac{V}{V_a} \cos\gamma - \frac{W_x}{V_a} \right) \right] \quad (13)$$

$$\Delta\dot{\gamma}' = \frac{\partial W_x}{\partial z} \left( \frac{V}{V_a} \right)^2 \sin^2\gamma \quad (14)$$

Figure 4 illustrates the variation of the wind shear contribution to the relative airspeed acceleration as a function of altitude for a conventional logarithmic wind speed profile given by

$$W_x = \frac{u_*}{\kappa} \ell n \frac{z + z_o}{z_o}$$

where the friction velocity $u_* = 1$ m/s and the surface roughness $z_o = 10^{-3}$ m. It is interesting to observe that the curves for a landing speed of 70 m/s at an angle of $-3$ deg are nearly coincident to the curve for a slower landing speed of 35 m/s and a steeper glide path of $-7$ deg. The former values are typical of the landing speed and glide path of a CTOL aircraft whereas the latter values are typical of those of a STOL aircraft. Figure 4 illustrates that the strong influence of wind shear suspected to occur for STOL aircraft is no worse than for CTOL aircraft because of the compensating effects of the steeper glide path. That is, even though the STOL aircraft has a slower landing speed, it "cuts" through velocity gradients at a rate equivalent to that of the CTOL aircraft because of the steeper glide slope.

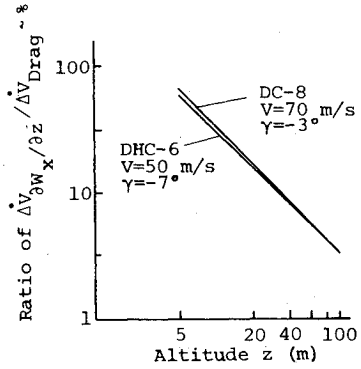


Fig. 6 Ratio of change in $V_a$ due to wind shear to that due to drag.

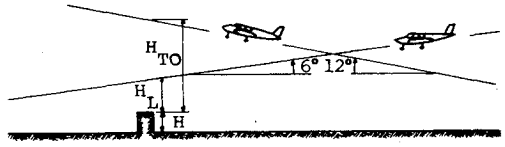


Fig. 7 Flight paths of STOL aircraft over a block building.

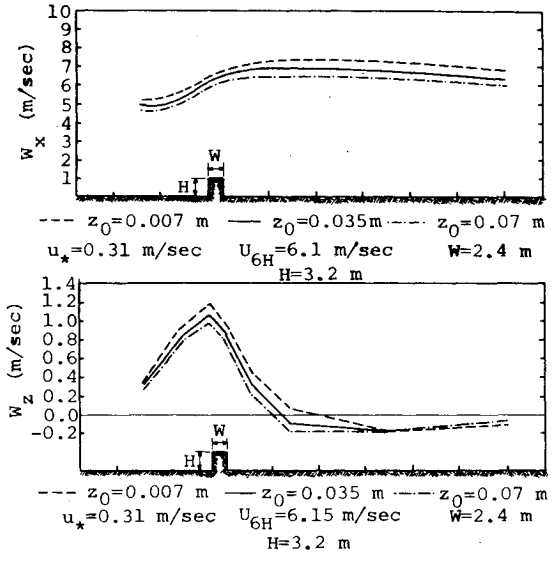


Fig. 8 Wind "seen" by aircraft landing over block building.

Figure 5 shows the contribution to the change of pitch angle caused by wind shear. Again, one sees that the competing effects of higher landing speed coupled with smaller glide slope and slower landing speed coupled with steeper glide slope tend to bring the curves for the rate of change of pitch rate close to one another.

It is also interesting to compare the contribution to the change of relative velocity caused by wind shear to that caused by drag. Taking the ratio of those two terms appearing in Eq. (8) and computing their effects for an atmospheric boundary layer, one obtains the results shown in Fig. 6. Once again, due to the variation in landing speed and glide slope, this ratio remains almost identical for the two different aircraft. Thus, one is led to believe that the suspected influence of wind shear on the STOL aircraft will not be as pronounced as originally suggested.[5,6] Similar conclusions regarding the influence of wind shear on STOL aircraft are reported by Ramsdell.[7]

## Flight through Building Disturbed Winds

Having introduced the effects of wind shear into the governing equations of motion for the airplane, the performance of aircraft in the wind fields created by atmospheric

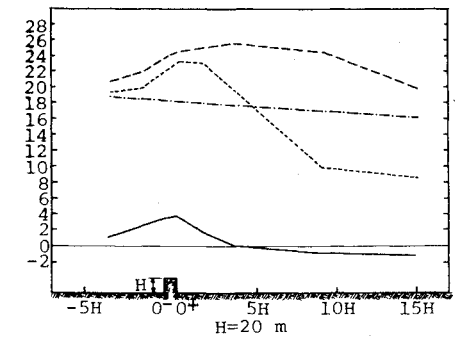


**Fig. 9 Wind speed "seen" by aircraft taking off over block building.**

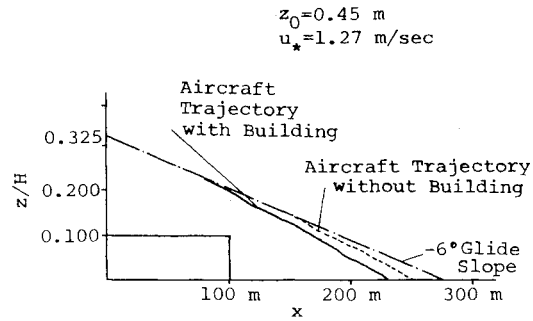


**Fig. 10 DHC-6 landing flight path over long, very wide, low building in a 10 m/s head wind.**

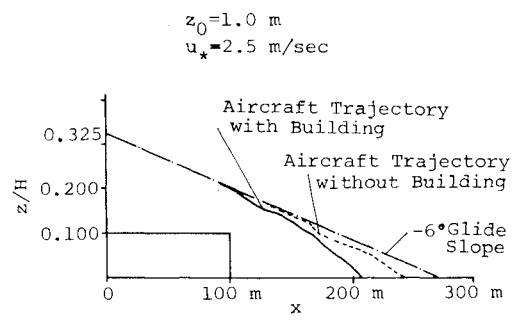


**Fig. 11 DHC-6 landing flight path over a long, very wide, low building in a 15 m/s head wind.**

flow over simulated buildings is investigated. Figure 7 shows the flight path of an aircraft taking off and landing into the wind flowing over a two-dimensional bluff-type body similar to a block building.

Figures 8 and 9 show typical wind fields that would be encountered by the aircraft if it remained on the prescribed flight path. The values of $u_*$ and $z_o$ given in the figure correspond to that of the undisturbed wind field upstream of the building. One observes, for landing into a flow over a building, a sudden drop in longitudinal wind speed just as the aircraft passes over the building and a sudden increase in vertical updraft. Figure 9 shows the wind encountered by an airplane on a fixed takeoff flight path. Again, one observes a rather severe increase in head wind as the airplane passes over the building. These wind fields are introduced into the equations of motion, and the results describing the computed flight paths of the airplane through the wind fields with both fixed and automatic controls are discussed below.

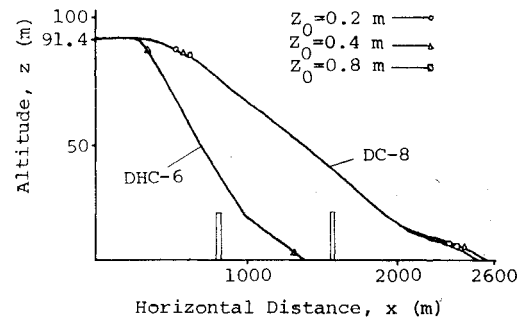


**Fig. 12 Automatic landings over block building. (Note: building on left for DHC-6; right for DC-8.)**

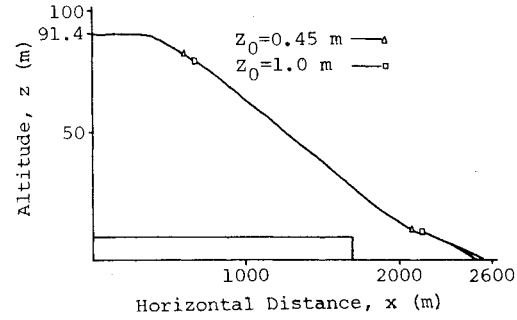


**Fig. 13 Automatic landing over a long, wide building.**

Figures 10 and 11 show the flight path of a STOL aircraft landing with fixed controls over a long, very wide, low building. Additionally, the flight path and the aircraft trajectory landing in an atmospheric boundary layer undisturbed by the presence of the building are illustrated. The sudden decrease in head wind encountered just at the leading edge of the building causes the airplane with fixed controls to land short. With a 10 m/s head wind, the airplane lands approximately 30 m short of the glide path touchdown point; with a 15 m/s head wind the aircraft lands approximately 70 m short. Thus, under strong wind conditions, the aircraft encountering a strong shear caused by the edge of the building is drawn in toward the building. This illustrates the potential hazard of the presence of large bluff objects which create complex wind patterns in approach paths.

In view of the fact that fixed control landings do not simulate authentic approaches, an automatic control system was introduced into the computer program. The automatic landing system uses thrust and elevator control output servomechanisms based on velocity and pitch rate inputs. The control outputs from the servomechanisms are determined from the following equations:

$$F_{T_C} = K_{T1} V_a + K_{T2} \frac{\dot{z}}{V} + K_{T3} \frac{\dot{x}}{V} + K_{T4} \theta_c \tag{15}$$

$$\delta_{E_C} = K_{E1} V_a + K_{E2} \frac{\dot{z}}{V} + K_{E3} \frac{\dot{x}}{V} + K_{E4} \theta_c \tag{16}$$

where the gains $K$ are evaluated during each time step of the landing by solving Eqs. (1, 2, and 3) simultaneously for $F_T$, $\alpha'$, and $\delta_E$.

This system appears to control the aircraft ideally through the variable wind fields over buildings (see Figs. 12 and 13). In fact, deviations from the expected touchdown point were decreased considerably (minimum 82% improvement) over simulations involving aircraft with fixed controls. However, the control inputs necessary to follow the desired flight path so closely are of primary importance. Figures 14 and 15 examine these inputs with respect to horizontal distance for flight over both the block and step geometries, respectively.

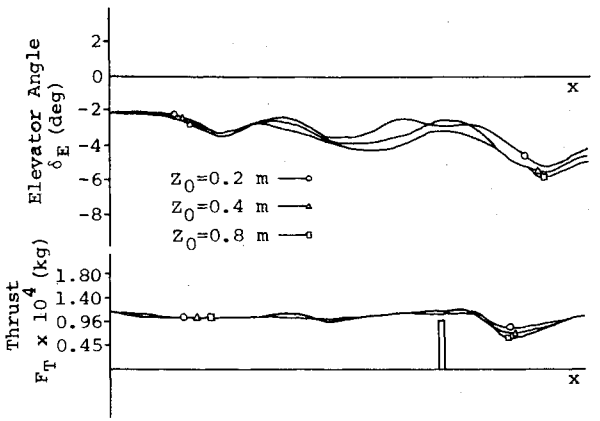


**Fig. 14 Controls required for landing over a block building.**

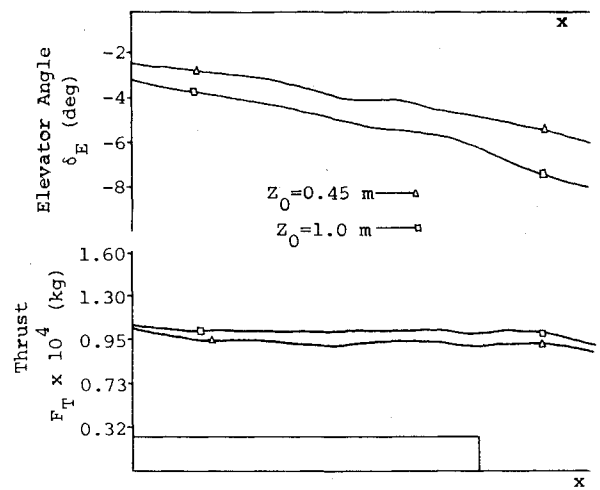


**Fig. 15 Controls required for landing over a step.**

Inspection of these figures shows the building effects to have significant influence on the control inputs. Thrust (Fig. 14) must be reduced significantly as the aircraft passes over the building to compensate for the sudden excursions in horizontal and vertical winds. Elevator angle is constantly changing to maintain a constant pitch rate. The control input for flight over a long, wide building (Fig. 15) shows that the elevator angle requires steady reduction (pitch up) as the aircraft lands. Also, abrupt change in thrust control is observed as the aircraft clears the building.

The automatic control system utilized in this study is idealized in terms of the feedback parameters employed; that is, some parameters used to calculate the inputs such as angle of attack, ground speed, etc., may not be readily obtainable from a standardly equipped aircraft.

## Conclusions

The two-dimensional, three-degrees-of-freedom aircraft landing simulation study has provided some basic results concerning the effects of wind shear on CTOL and STOL aircraft operations in the presence of large buildings and other bluff geometries. The aircraft encountering a strong wind shear, caused by the edge of a building, is drawn toward the building. Thus, a hazardous situation results due to departure from the intended touchdown point. Recommendations concerning these types of operations under given wind conditions will require more simulations (i.e., a sufficient number to find hazard reduction criteria) and analysis of the complex flowfields around such structures.

## Acknowledgments

The authors are grateful for the support of J. Enders of the Aviation Safety Technology Branch, Office of Aeronautics and Space Technology (OAST); and G. H. Fichtl, Chief of Fluid Dynamics Branch, Atmospheric Sciences Division, George C. Marshall Space Flight Center, Ala.

## References

[1] Fichtl, G.H., Camp, D.W., and Frost, W., "Sources of Low-Level Wind Shear around Airports," *Journal of Aircraft*, Vol. 14, Jan. 1977, pp. 5-14.

[2] Bitte, J. and Frost, W., "Atmospheric Flow over Two-Dimensional Bluff Surface Obstructions," NASA CR-2750, Oct. 1976.

[3] Shieh, C.F., Frost, W., and Bitte, J., "Neutrally Stable Atmospheric Flow over a Two-Dimensional Rectangular Block," Report prepared under NASA Contract NAS8-29584, Univ. of Tennessee Space Institute, Tullahoma, Tenn., NASA CR-2926, Nov. 1977.

[4] Frost, W. and Reddy, R., "Investigation of Aircraft Landing in Variable Wind Fields," NASA Contractor Rept. 3073, Dec. 1978.

[5] "STOL Technology," NASA SP-320. Conference held at Ames Research Center, Moffett Field, Calif., Oct. 17-19, 1972.

[6] "Flight in Turbulence," AGARD-CP-140. Symposium of the 42nd Meeting of the Flight Mechanics Panel of AGARD held at Woburn Abbey, Bedfordshire, England, May 14-17, 1973.

[7] Ramsdell, J.V., "Wind Shear Fluctuations at a Typical Urban V/STOL Port Site," Sixth Conference on Aerospace and Aeronautical Meteorology of the American Meteorological Society, El Paso, Texas, Nov. 12-15, 1974.